3.1 P_a and R_t for triangular input function

Suppose that sources are triangular stress pulses which originate and arrive at the transducer input at time $t = 0$. The output due to such a stress pulse is given by (16) from which we get the peak amplitude P_a (i.e. max $g_T(t)$) as

$$P_a = CAT \int_{f1}^{f2} \frac{\sin^2(\Pi fT/2)}{(\Pi fT/2)^2} \, df. \tag{20}$$

Similarly, the rise time R_t is given by

$$R_t = T/2. \tag{21}$$

Equations (20) and (21) are proved in appendix A.

3.2 P_a and R_t for gaussian input function

The output signal for Gaussian stress pulses (figure 7) is given by (17). P_a of this signal is given by

$$P_a = \max g_G(t) = 2\sqrt{(2\Pi)}CA\sigma \int_{f1}^{f2} exp[-\sigma^2 4\Pi^2 f^2/2] \, df. \tag{22}$$

Equation (22) can be proved along the same lines as (20). P_a occurs uniquely at $t = t_0 + 3\sigma$. Uniqueness of P_a can also be proved by the same line of arguments as for the triangular function.

If we take, as in the case of the triangular input function, time origin as the instant when the signal first appears at the transducer output, i.e., treating $t_0 = 0$, we get R_t measured from the origin as

$$R_t = 3\sigma.$$

Since the total duration or pulse width of the Gaussian pulse (figure 7) is $T = 6\sigma$. Hence the equation $R_t = 3\sigma$ states that R_t as measured from the beginning of the signal is equal to half the pulse width T. That is,

$$R_t = T/2. \tag{23}$$

This relationship between R_t and T is the same as that between them in the case of the triangular input, (21).

3.3 P_a and R_t for rectangular and half cosine input functions

The output signal due to the rectangular input of figure 9 is given by (18). If the pulse width T and the upper cut-off frequency f_2 are such that $f_2T \le 1$, i.e. $\Pi f_2T \le \Pi$ for all f, $f_1 \le f \le f_2$, then $\sin \Pi ft/\Pi ft \ge 0$. Under this condition a closed-form expression for P_a and R_t analogous to those for triangular and Gaussian input functions can be obtained as

$$P_a = \max g_R(t) = 2CAT \int_{f1}^{f2} \frac{\sin \Pi fT}{\Pi ft} \, df, \tag{24}$$

and

$$Rt = T/2. \tag{25}$$

The output signal for half cosine input function of figure 10 is given by (19) and the function $\cos \Pi f T / \left[(\Pi / T)^2 - (2\Pi f)^2 \right]$ takes the positive maximum value when $\Pi f T = 0$, and crosses zero first when $\Pi f T = 3\Pi/2$.

Suppose that T and f_2 are such that

$$\Pi f_2 T \le 3\Pi/2, \text{ i.e. } f_2 \le 3/2T \text{ or } T \le 3/2 f_2.$$

Under this condition $\cos \Pi f T / \left[(\Pi / T)^2 - (2\Pi f)^2 \right] \ge 0$ for all f, $f_1 \le f \le f_2$ and hence P_a is given by

$$P_a = \frac{4 C A \Pi}{T} \int_{f1}^{f2} \cos \Pi f T / (\Pi / T)^2 - (2\Pi f)^2 \, \mathrm{d} f, \tag{26}$$

and

$$R_t = T/2. \tag{27}$$

In (25) and (27), it is assumed that the time origin is the instant when the signal first appears at the transducer output.

4. Verification using simulated signals

Results given by (20), (22), (24) and (26) and the relation $R_t = T/2$ do not exist, to the best knowledge of the present authors, in signal processing, control system, or any other related technical literature. In order to ascertain the validity of these equations, we simulated signals by numerically integrating (16)–(19). The procedure adopted is the Gauss–Legendre quadrature formula which is one of the most accurate numerical integration procedures. Gauss–Legendre approximation for the integral of any function $f(x)$ over the interval $(-1, 1)$ is given by (Krylov 1966),

$$\int_{-1}^{1} f(x) \mathrm{d} x \approx \sum_{i=1}^{N} w_i f(\lambda_i), \tag{28}$$

where N is the number of points or nodes, (λ_i) the zeros of the Legendre polynomial of degree N, and $[w_i]$ the appropriate weight factors. $\int_a^b f(x) \mathrm{d} x$ can be obtained from $\int_{-1}^{1} f(x) \mathrm{d} x$ by the transformation i.e.

$$\int_a^b f(x) \mathrm{d} x = \frac{b - a}{2} \int_{-1}^{1} f \left[\frac{b - a}{2} y + \frac{a + b}{2} \right] \mathrm{d} y.$$

The values $f_1 = 250$ kHz and $f_2 = 500$ kHz were mainly used to simulate the signals using (16)–(19), the integrals were evaluated at equidistant points of 0.5 microseconds for a maximum value of 100 microseconds. Transducer parameters defined in (10) were chosen as $f_1 = 250$ kHz, $f_2 = 500$ kHz, $C = 1$ volt per microbar and $t_0 = 0$. The number of nodes $N = 512$ was found to be adequate because as N is increased from 48 to 512, the resulting
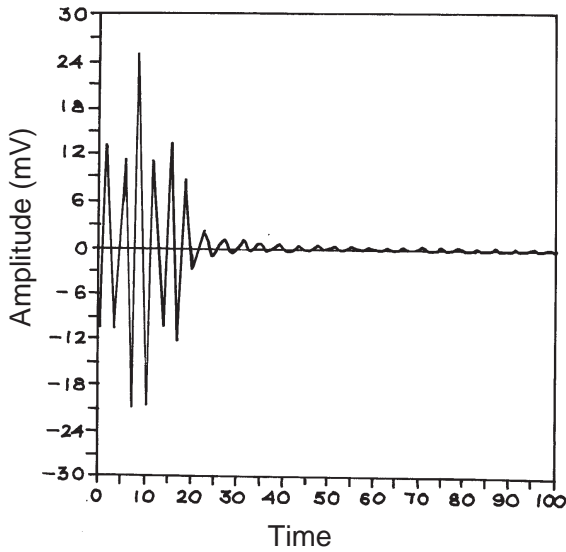
Figure 11. Signal due to a triangular source $T = 17$ microseconds and $A = 1$ microbar.

improvement in accuracy is not significant. $[\lambda_i]$ and $[w_i]$ were obtained as per Stroud & Secrest (1966).

Large data bases of signals were simulated by using these four stress pulses, viz., triangular, Gaussian, rectangular and half cosine for three different pulse heights, viz., 1, 2, and 3 microbar and pulse widths varying from 1 to 30 microseconds. Four typical examples of these signals are shown in figurs 11–14.

Peak amplitude for triangular and Gaussian input pulses obtained by numerically integrating (20) and (22) were found to be the same as the peak amplitude of simulated signals, simulated using these input functions, there by proving the validity of these equa-
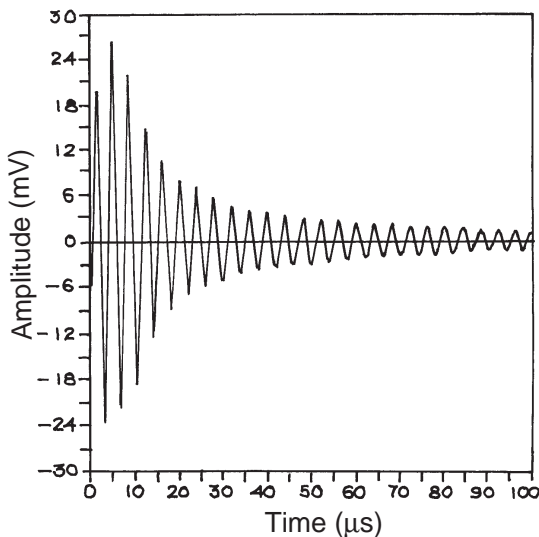

Figure 12. Signal due to a Gaussian source $T = 10$ microseconds and $A = 3$ microbar.

5. Significance of peak amplitude and rise time

The relation that pulse width is twice the rise time and the equations for peak amplitude, (20), shows that rise time and peak amplitude contain complete information about triangular source parameters. This is obvious from (20) which can be written, by rearranging and substituting $R_t = T/2$, as

$$A = Pa/\left[CT \int_{f1}^{f2} \frac{\sin^2(\Pi f\ R_t)}{(\Pi f R_t)^2}\ \mathrm{d}f \right]$$

This is true about Gaussian, rectangular (under the condition $f_2 \leq 1/T$), and half cosine (under the condition $f_2 \leq 3/2T$) inputs. In brief, we can conclude from the foregoing that peak amplitude and the rise time are significant parameters for source characterization.

6. Conclusion

Theoretical expressions for peak amplitude and rise time of acoustic emission signals are derived. Correctness of these expressions are established using simulated signals. Inferences drawn from these expressions justify the use of these parameters for acoustic emission source characterization.

Appendix A

From (16) we get

$$g_T(t) \leq CAT \int_{f1}^{f2} |\frac{\sin^2(\Pi f T/2)}{(\Pi f T/2)^2} \cos 2\Pi f[t - (t_0 + T/2)]|\ \mathrm{d}f$$

$$\leq CAT \int_{f1}^{f2} \frac{\sin^2(\Pi f T/2)}{(\Pi f T/2)^2}| \cos 2\Pi f[t - t_0 + T/2)]|\ \mathrm{d}f$$

$$\leq CAT \int_{f1}^{f2} \frac{\sin^2(\Pi f T/2)}{(\Pi f T/2)^2}\ \mathrm{d}f, \tag{A1}$$

$$\frac{\mathrm{d}g_t(t)}{\mathrm{d}t} = CAT \int_{f1}^{f2} \frac{\sin^2(\Pi f T/2)}{(\Pi f T/2)^2}\ (\mathrm{d}/\mathrm{d}t)\{\cos 2\Pi f[t - (t_0 + T/2)]\}\mathrm{d}f,$$

that is,

$$\frac{\mathrm{d}g_T(t)}{\mathrm{d}t} = -2CAT \int_{f1}^{f2} \frac{\sin^2(\Pi f T/2)}{(\Pi f T/2)^2}\ \sin 2\Pi f[t - (t_0 + T/2)]\Pi f\mathrm{d}f,$$

$$\frac{\mathrm{d}^2 g_T(t)}{\mathrm{d}t^2} = -4CAT \int_{f1}^{f2} \frac{\sin^2(\Pi f T/2)}{(\Pi f T/2)^2}\ \cos 2\Pi f[t - (t_0 + T/2)](\Pi f)\mathrm{d}f,$$

$$\frac{\mathrm{d}g_T(t)}{\mathrm{d}t} = 0 \text{ when } t = t_0 + T/2,$$

and

$$\frac{\mathrm{d}^2 g_T(t)}{\mathrm{d}t} < 0 \text{ at } t = t_0 + T/2.$$

Hence $g_T(t)$ has a maximum at $t = t_0 + T/2$ which is given by

$$gT(t_0 + T/2) = CAT \int_{f1}^{f2} \frac{\sin^2(\Pi f T/2)}{(\Pi f T/2)^2} \, \mathrm{d}f. \tag{A2}$$

By comparing (A2) with (A1) we find that $g_T(t)$ attains its upper bound, given by (A1), at $t = t_0 + T/2$ thus completing the proof.

Assume that we have a $t = t' \neq t_0 + T/2$ such that $g_T(t') = \max g_T(t) = P_a$. This implies that $\cos 2\Pi f[t' - (t_0 + T/2)] = 1$, for all $f_1 \leq f \leq f_2$ (otherwise $g_T(t') < CAT \int_{f1}^{f2}\{[\sin^2(\Pi f T/2)]/(\Pi f T/2)^2\} \, \mathrm{d}f = P_a$) implying that $2\Pi f[t - (t_0 + T/2)] = 0$ for all $f_1 \leq f \leq f_2$. This is impossible and hence, our assumption is wrong and P_a occurs uniquely at $t = t_0 + T/2$.

We have seen that P_a occurs at $t = t_0 + T/2$. Suppose we treat the instant when the signal first appears at the transducer output as the time origin. This is equivalent to treating the instant when the transient pulse is applied to the transducer as the time origin with $t_0 = 0$. Under this condition we get

$$R_t = T/2. \tag{A3}$$

References

Bhat M R, Murthy C R L 1993 Fatigue damage stages in unidirectional glass-fibre-epoxy composites: Identification through acoustic emission technique. *Int. J. Fatigue* 15: 401–405

Hill R, Stephens R W B 1974 Simple theory of acoustic emission–a consideration of measurement parameters. *Acoustica* 31: 225–230

Krylov V I 1966 *Approximate calculation of integrals* (NewYork: MacMillan)

Murthy C R L, Majeed M A, Pathak S C, Rao A K 1985 In-Flight monitoring for incipient cracks in an aero engine mount: An approach through pattern recognition. *J. Acoust. Emission* 4: S147–S150

Murthy C R L, Dattaguru B, Rao A K 1987 Application of pattern recognition concepts to acoustic emission signal analysis. *J. Acoust. Emission* : 19–28

Papoulis A 1977 *Signal analysis* (New Delhi:McGraw-Hill)

Salivahanan S, Vallavaraj A, Gnanapriya C 2000 *Digital signal processing* (New Delhi: Tata McGraw-Hill)

Stephens R W B, Pollock A A, 1971 Waveforms and frequency spectra of acoustic emission. *J. Acoust Soc. Am.* 50: 904-910

Stroud A H, Secrest D 1966, *Gaussian quadrature formulas* (Englewood Cliffs, NJ: Prentice-Hall)